



Freeze–thaw processes correspond to the protection–loss of soil organic carbon through regulating pore structure of aggregates in alpine ecosystems

Ruizhe Wang^{1,2} and Xia Hu^{1,2}

¹State Key Laboratory of Earth Surface Process and Resource Ecology, Faculty of Geographical Science, Beijing Normal University, Beijing 100875, China

²School of Natural Resources, Faculty of Geographical Science, Beijing Normal University, Beijing 100875, China

Correspondence: Xia Hu (huxia@bnu.edu.cn)

Received: 16 June 2024 – Discussion started: 8 July 2024

Revised: 16 October 2024 – Accepted: 18 October 2024 – Published: 4 December 2024

Abstract. Seasonal freeze–thaw processes alter soil formation and lead to changes in soil structure of alpine ecosystems. Soil aggregates are basic soil structural units and play a crucial role in soil organic carbon (SOC) protection and microbial habitation. However, the impact of seasonal freeze–thaw processes on pore structure and their impact on SOC fractions have been overlooked. This study characterized the pore structure and SOC fractions of soil aggregates of the unstable freezing period, stable frozen period, unstable thawing period and stable thawed period in typical alpine ecosystems via a dry-sieving procedure, X-ray computed tomography scanning and elemental analysis. The results showed that pore networks of 0.25–2 mm aggregates were more vulnerable to seasonal freeze–thaw processes than those of > 2 mm aggregates. The freezing process promoted the formation of > 80 µm pores of aggregates. The total organic carbon, particulate organic carbon and mineral-associated organic carbon contents of aggregates were high in the stable frozen period and dropped dramatically in the unstable thawing period, demonstrating that the freezing process was positively associated with SOC accumulation, while SOC loss featured in the early stage of thawing. The vertical distribution of SOC of aggregates was more uniform in the stable frozen period than in other periods. Pore equivalent diameter was the most important structural characteristic influencing SOC contents of aggregates. In the freezing period, the SOC accumulation might be enhanced by the formation of > 80 µm pores. In the thawing period, pores of < 15 µm were positively correlated with SOC concentration. Our results revealed that changes in pore structure induced by freeze–thaw processes could contribute to SOC protection of aggregates.

1 Introduction

The alpine regions contribute to over 50 % of the soil organic carbon (SOC) stock in terrestrial ecosystems, which is 1.5 times greater than the atmospheric carbon pool (Tarnocai et al., 2009). Significant carbon emissions from warming-induced permafrost thawing could further provide a positive carbon feedback to climate change (Schuur and Mack, 2018). Freeze–thaw (FT) cycles are the main processes of soil formation in alpine regions (Wang et al., 2007). Ongoing global warming has reduced snow cover in winter and decreased the

insulation of soils against freezing, which has increased the frequency of FT cycles (Kreyling et al., 2007). Soil aggregates are fundamental soil structural units and favour SOC protection (Oztas and Fayetorbay, 2003; Tan et al., 2014). SOC is preserved by physical protection in the forms of particulate organic carbon (POC) and mineral-associated organic carbon (MAOC). POC is a crucial contributor to soil aggregation and parallels plant-derived carbon in aggregates, and MAOC plays a crucial role in long-term SOC storage (Wang et al., 2020; Witzgall et al., 2021). FT processes may loosen the aggregates' protection of SOC by stimulating sub-

strate release (Song et al., 2017), destroying aggregate stability and stimulating microbial activities (Campbell et al., 2014; Xiao et al., 2019), and the impact is highly dependent on SOC components. For example, FT processes could significantly increase soil soluble carbon content and extractable SOC content but decrease the microbial biomass carbon (MBC) content of aggregates (Patel et al., 2021). The increase in microporosity and microbial activities in aggregates induced by FT could decrease the dissolved organic carbon (DOC) concentration (Kim et al., 2023). More frequent FT processes enhance SOC availability, especially in active layers, and thus lead to a high risk of greenhouse gas release (Estop-Aragónés et al., 2020). However, these related studies were mostly based on simulated laboratory FT experiments. The field FT process is elusive as it contains the complex interactions between soil properties, plant growth and topographic features, and these lead to differences in the outcomes between laboratory and field measurements (Henry, 2007; Deng et al., 2024). Therefore, quantifying the actual dynamics of SOC of aggregates under seasonal FT processes is valuable.

Soil structure refers to the spatial arrangement of solids and voids and controls many important biophysical processes in soils (Rabot et al., 2018). The pore networks of soil aggregates are heterogeneous. FT processes not only affect the stability of soil aggregates but also alter their inner pore characteristics, especially those of the water-filled pores (Wang et al., 2012; Li and Fan, 2014; Starkloff et al., 2017). A decrease in pore connectivity, an increase in elongated porosity and an increase in asymmetrical pores were observed after continuous FT events (Ma et al., 2021; Rooney et al., 2022; Kim et al., 2023). The pore network determines the accessibility of organic matter to microbes and indirectly influences microbial activities, thus determining the magnitude to which the SOC is protected (Ruamps et al., 2013; Kravchenko and Guber, 2017). Interactions between pore structure and SOC fractions of soil aggregates have gained much attention. Pores of 30–75 and > 13 µm in size were found to enhance the carbon mineralization (Lugato et al., 2009; Kravchenko et al., 2015). Pores of > 90 and < 15 µm in size were found to support SOC protection (Ananyeva et al., 2013; Quigley and Kravchenko, 2022). Pores of 30–150 µm are also the preferential places for new carbon inputs, and greater abundance of such pores translates into a higher spatial footprint that microbes make on SOC storage capacity (Kravchenko et al., 2019). These distinct correlations demonstrated that the pore–SOC interactions are highly dependent on environmental conditions. In alpine ecosystems, the dynamics of SOC can be significantly associated with the transformation and destruction of aggregates induced by FT processes (Dagesse, 2013). However, the role of pore structure in regulating SOC dynamics in FT processes has not been revealed.

The Qinghai–Tibetan Plateau (QTP) has warmed at twice the global average rate in recent years, with the average temperature being expected to increase by over 2 °C before 2070

(Lin et al., 2019). Soils of the QTP are fragile and vulnerable to global climate change. The depth and duration of FT processes have decreased, while the frequency of FT cycles has increased in the QTP (Peng et al., 2017), posing dramatic alterations on the soil pore network (Gao et al., 2021; Yang et al., 2021). Previous studies have shown that alpine meadow soil aggregates of the QTP had dense pore networks with many elongated pores due to frequent FT cycles (Zhao et al., 2020). For typical ecosystems on the QTP, the aggregate protection of SOC was promoted by pores of < 15 µm via limiting microbial access, and the process was most closely associated with soil moisture content (Wang and Hu, 2023). Aggregate stability has been proved to impact SOC protection on the QTP, and thawing-induced SOC loss of aggregates will translate into carbon emissions from the meadow to the atmosphere and exacerbate global warming (Ozlu and Arriaga, 2021). Changes in carbon storage depend on relationships between SOC input from litter and root exudates and output by microbial metabolic activities, and pore structure defines the pathway of substrate movement (Qiao et al., 2023). Overall, the pore structure of aggregates under FT conditions has important implications for predicting carbon turnover projections under global warming (He et al., 2021).

To fill these research gaps, the objectives of the study were as follows: (1) to quantify changes in pore structure and SOC fraction contents of aggregates in typical alpine ecosystems during the seasonal FT process, (2) to investigate the relationships between them, and (3) to clarify the role of pore structure in aggregate functions related to SOC protection during seasonal FT processes.

2 Materials and methods

2.1 Study sites and sampling

The study was carried out in the Qinghai Lake watershed (36°15′–38°20′ N, 97°50′–101°20′ E), northeastern QTP. The area lies in the cold and high-altitude climate zone, with a mean annual temperature and precipitation of 0.1 °C and 400 mm, respectively (Li et al., 2018). Two ecosystems were selected in the study: *Kobresia pygmaea* meadow (KPM) and *Potentilla fruticosa* shrubland (PFS) (Fig. 1). They are representative terrestrial ecosystems of the Qinghai Lake watershed and account for over 60 % of the total watershed land area (Hu et al., 2016). One of the main features of these two ecosystems is the mattic epipedon present on the soil surface. Mattic epipedon is the surface layer consisting of a grass felt-like complex formed by the interweaving of live and dead roots of different ages. The layer is soft and significantly enhances nutrient preservation (Hu et al., 2023). The soil type was classified as Gelic Cambisols according to the FAO UNESCO system (IUSS Working Group WRB, 2022). We tried to avoid the simple pseudo-replication; therefore each sampling site has a certain distance from others (> 1 km). Three sites within each ecosystem have similar

vegetation conditions. In every FT period, three sampling plots (1 m × 1 m) were set up at each site.

The division of seasonal FT periods is based on changes in daily soil temperature of the whole soil profile (Chen et al., 2021; Wu et al., 2023). The EM-50 soil temperature data for 2019, 2020 and 2021 were obtained at 0.5 Hz with 30 min averages at all three study sites using the ECH2O 5TE sensor (Decagon Devices, USA) (Li et al., 2018). The seasonal FT process was divided into four periods in this study (Fig. 2): the unstable freezing period (UFP; as soil temperature starts to drop to 0 °C), the stable frozen period (SFP; with soil temperature completely below 0 °C), the unstable thawing period (UTP; as soil temperature starts to rise above 0 °C) and the stable thawed period (STP; with soil temperature completely above 0 °C). The freezing process included the SFP and UFP, while the thawing process included the STP and UTP. Soil samples were taken in October 2021 (representing UFP), January 2022 (representing SFP), May 2022 (representing UTP) and July 2022 (representing STP).

Soils from three typical profiles in the sampling plots (1 m × 1 m) were dug at each site. A total of 18 soil profiles were obtained in every FT period. We classified the soil layers as 0–10, 10–30 and 30–50 cm soil layers. Soil cores and bulk soil were collected at each soil layer for aggregate sieving and physiochemical characteristic measurements, respectively. Soil cores were obtained using a 70 mm diameter soil auger and then preserved in an icebox before being sieved in the laboratory. A total of 54 soil cores were collected in every FT period. Nitrile powder-free gloves, a plastic garden trowel and a small saw were utilized for bulk soil sampling. The basic soil properties of each soil layer at the study site are listed in Table S1 in the Supplement. Particle size distribution was determined using the sieve–pipette method (Mako et al., 2019). The soil water content as weight was determined using an oven-dried method (Klute, 1986). Soil pH measurements were conducted by an FE20 pH meter (Mettler Toledo, Columbus, USA) from slurries of samples at a soil-to-water ratio of 1 : 2.5 (*w* : *w*) (Zhao et al., 2020). SOC and total nitrogen (TN) contents were determined using a CN 802 elemental analyser (VELP, Italy). Inorganic carbon was removed from the soil samples using 1 mol L⁻¹ HCl prior to elemental analysis (Zhang et al., 2017).

2.2 Aggregate sieving

Separation of soil aggregates was performed using the dry-sieving method with 0.053, 0.25 and 2 mm sieves from bottom to top. Soil cores were gently broken by hand into 1 cm clods, and then soils were laid out between sheets of brown paper (Schutter and Dick, 2002). Debris such as gravel and roots was removed from the samples. A quantity of 200 g of soil was placed on the top sieve and was shaken for 5 min by the sieve shaker (200 rpm). The aggregates were divided into four categories: large macroaggregates (LMAs; with diameters > 2 mm), small macroaggregates (SMAs; with diam-

eters of 0.25–2 mm), microaggregates (mAs; with diameters of 0.053–0.25 mm) and fractions with diameters < 0.053 mm (Li et al., 2022). Aggregate fractions of > 2 and 0.25–2 mm were weighed and preserved for further analysis.

2.3 CT scanning and image processing

A nanoVoxel-4000 X-ray three-dimensional (3D) microscopic CT (Sanying Precision Instruments Co., Ltd., China) was used to scan the soil aggregates with X-ray source parameters of voltage 80 kV and current 50 μA, with which 2800 detailed and low-noise images could be obtained during a 360° rotation. The reconstructed images featured a 3.6 μm spatial resolution and 2800 × 2800 × 1500 voxels. Aggregate fractions of > 2 and 0.25–2 mm from all soil layers of the UFP, SFP, UTP and STP periods were scanned (other fractions were too small to separate into a single sample). A total of 144 aggregates were selected and scanned.

Reconstruction of the pore network of aggregates was completed using Avizo 9.0 (Visualization Sciences Group, Burlington, MA). The procedure for image analysis was similar to that described by Wang and Hu (2023) (Fig. 3). Briefly, the clutters around the aggregates were eliminated using the “Volume Editing” module. Mask extraction was carried out in the Segmentation module (Zhao et al., 2020). The soil matrix was selected with the “Magic Wand” tool, and then the “Fill” tool was used to fill the pores for obtaining the aggregate boundary and the mask of the whole aggregate (Zhao and Hu, 2023a). All images were segmented in a binary way using the histogram thresholding method based on the global thresholding algorithm (Jaques et al., 2021), and pore thresholds were selected for all images.

The intra-aggregate porosity was calculated using the “Volume Fraction” tool. The two-dimensional images were transformed into 3D images by the “Volume Rendering” tool in Avizo 9.0 software. After the transformation, pore characteristics including the equivalent diameter, volume, length, shape factor and surface area were calculated using the “Label Analysis” tool.

One pore network may consist of several branches of connected pores or just one individual pore. The pore length is the total actual length in all branches. The pore length density (LD) is defined as the ratio of the pore length (*L*) to the total volume of pores (*V*) (Yang et al., 2021):

$$LD = \frac{L}{V}. \quad (1)$$

The surface area density (SD) is defined as the ratio of the pore surface area (*S*) to the total volume of *V*:

$$SD = \frac{S}{V}. \quad (2)$$

To characterize the pore shape, the pore shape factor (SF) was calculated as follows:

$$SF = \frac{A_0}{A}, \quad (3)$$

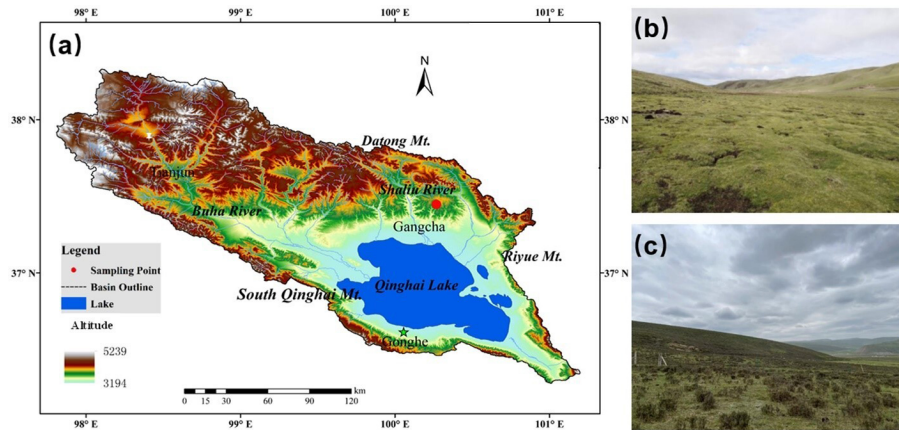


Figure 1. Location of the sampling site (a) and landscapes of the *Kobresia pygmaea* meadow ecosystem (b) and the *Potentilla fruticosa* shrub ecosystem (c).

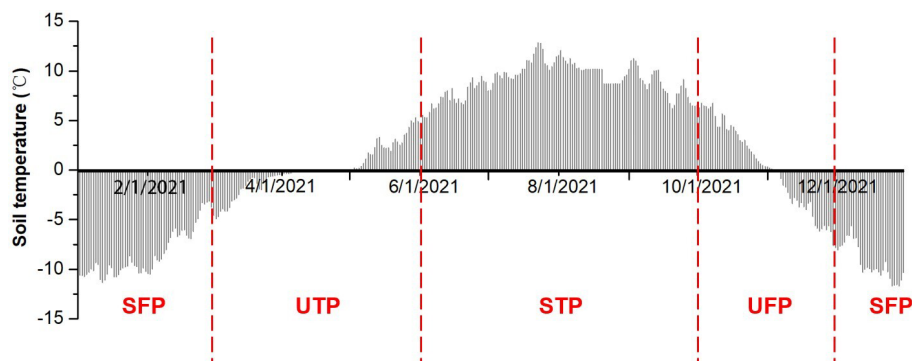


Figure 2. Daily average soil temperature in 2021 and the classification of freeze–thaw stages (SFP – stable frozen period, UTP – unstable thawing period, STP – stable thawed period and UFP – unstable freezing period).

where A_0 represents the surface area of the equivalent sphere of the pores, and A is the actual surface area of the pores. SF values closer to 1 indicate a more regular pore shape (i.e., closer to a spherical shape), and smaller values refer to more irregular or elongated pore shapes (Zhou et al., 2012).

The equivalent diameter (EqD) was defined as the diameter of spherical particle with the same volume and was calculated by pore volume:

$$\text{EqD} = \sqrt[3]{\frac{6 \times V}{\pi}}, \quad (4)$$

where V represents the volume of pores.

The pores were divided into four classes based on their equivalent diameter: < 15, 15–30, 30–80 and > 80 μm . According to Lal and Shukla (2004) and Wang and Hu (2023), pores < 30, 30–80 and > 80 μm are termed micropores, mesopores and macropores, respectively.

2.4 SOC fraction separation

In every FT period, soil aggregate samples were sufficiently ground to pass through a 0.15 mm sieve before their total or-

ganic carbon content (TOC) content was measured using the CN 802 elemental analyser (VELP, Italy).

The determination of SOC fractions, including POC and MAOC, was performed as described by Cambardella and Elliott (1992). Approximately 5 g of each dried aggregate of the > 2 and 0.25–2 mm aggregate fractions was moved to a 50 mL centrifuge tube and dispersed in 25 mL of a sodium hexametaphosphate (0.5%, w/v) solution by shaking for 18 h in a reciprocating shaker at 120 rpm to ensure that it was evenly blended (Chen et al., 2020; Fu et al., 2023). The dispersed samples were rinsed onto a 53 μm sieve to separate MAOC (particle size < 53 μm) and POC (particle size > 53 μm) using distilled water until the water stream was clear and free of fine soil particles. After that, samples were transferred to evaporating dishes and dried at 65 $^{\circ}\text{C}$ for 48 h to isolate soils that solely contained POC or MAOC fractions (Six et al., 1998). After weighing and sieving, all the fractions' SOC contents were measured using the CN802 elemental analyser (VELP, Italy). The POC and MAOC contents were obtained by multiplying the percentage of each particle size fraction in the soil (Sun et al., 2023).

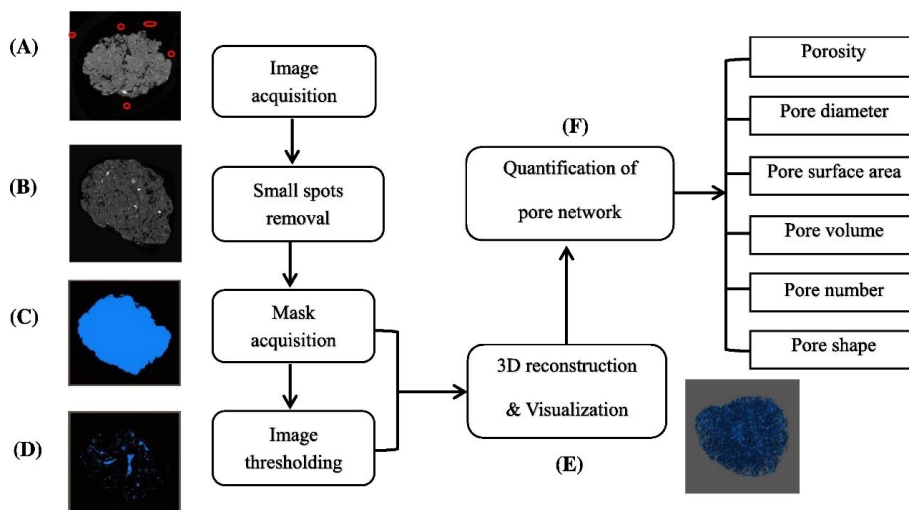


Figure 3. Procedures used for the visualization and quantification of soil aggregate pore networks. Taken from Zhao et al. (2020) with permission from Elsevier.

2.5 Statistical analysis

All statistical analyses except redundancy analysis (RDA) were conducted with IBM's SPSS 20 software (SPSS Inc., USA). One-way analysis of variance (ANOVA) followed by Fisher's protected least-significance difference (LSD) test was conducted to compare differences between the four seasonal FT periods and between different aggregate fractions. Pearson's correlations were conducted to evaluate the linkages between pore characteristics and SOC fractions of aggregates. Statistical significance was defined at $p < 0.05$. RDA was conducted to determine pore parameters that had a significant impact on SOC fractions and was carried out in R software (<http://www.r-project.org>, last access: 29 November 2024, version 4.0.2) using the vegan package.

3 Results

3.1 Pore characteristics of soil aggregates

Figure 4 depicts the pore size distribution of soil aggregates during the seasonal FT process. In the two ecosystems, pores of $> 80 \mu\text{m}$ dominated the pore space in all periods and accounted for over 65 % of the total porosity. The volume percentage of pores of $< 15 \mu\text{m}$ was low in the stable frozen period, with 4.39 % in the meadow ecosystem and 5.36 % in the shrubland ecosystem. The volume percentage of pores of $> 80 \mu\text{m}$ was high in the stable frozen period (80.62 % in the meadow ecosystem and 87.65 % in the shrubland ecosystem). The results showed that the freezing process increased the proportions of pores of $> 80 \mu\text{m}$, while thawing contributed to the increase in volume percentage of pores of $< 15 \mu\text{m}$.

The characteristics of the pores of aggregates during the seasonal FT process are shown in Fig. 5. The seasonal FT process did not significantly alter the porosity, pore volume and EqD (Fig. 5a, b and c). In the two ecosystems, significant variations were found in the mean pore volume between > 2 and 0.25–2 mm aggregates ($p < 0.05$). For 0.25–2 mm aggregates, the pore surface area density and length density in the thawing process were found to be significantly higher than those in the freezing process ($p < 0.05$), while no obvious trend was found for > 2 mm aggregates (Fig. 5d and e). Overall, seasonal FT processes are mainly associated with changes in the pore characteristics of 0.25–2 mm aggregates rather than those of > 2 mm aggregates.

3.2 SOC fraction contents of aggregates

The SOC fraction contents (TOC, POC and MAOC) of aggregates during the seasonal FT process are shown in Fig. 6. Generally, in the two ecosystems, the TOC contents of aggregates peaked in the stable frozen period, ranging from 57.33 to 60.28 g kg^{-1} (Fig. 6a). The following unstable thawing period demonstrated the dramatic decline in TOC contents of > 2 mm (dropped by 37.73 % and 32.95 % in the meadow and shrubland ecosystems, respectively) and 0.25–2 mm aggregates (dropped by 45.57 % and 39.43 % in the meadow and shrubland ecosystems, respectively) ($p < 0.05$).

Changes in contents of POC and MAOC were similar to those of TOC (Fig. 6b and c). In the meadow ecosystem, the POC contents were high in the stable frozen period (27.90 g kg^{-1} for > 2 mm aggregates and 33.77 g kg^{-1} for 0.25–2 mm aggregates), and a dramatic decline existed in the unstable thawing period (32.69 % for > 2 mm aggregates and 58.01 % for 0.25–2 mm aggregates) (Fig. 6b) ($p < 0.05$). The MAOC content of > 2 mm aggregates was

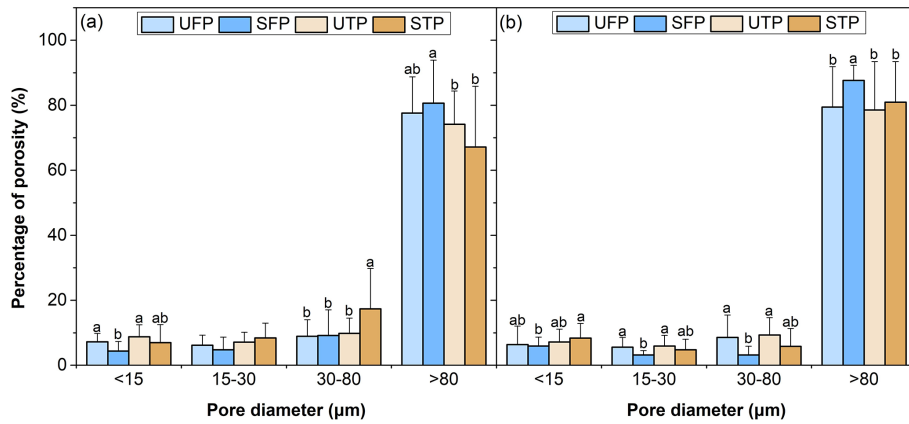


Figure 4. Pore size distribution (by pore diameter) of soil aggregates in the (a) meadow ecosystem and (b) shrubland ecosystem during the seasonal FT process. Bars represent the mean ± standard error ($n = 18$). Different lowercase letters denote significant differences among pore volume percentages in different FT periods ($p < 0.05$). UFP: unstable freezing period. SFP: stable frozen period. UTP: unstable thawing period. STP: stable thawed period.

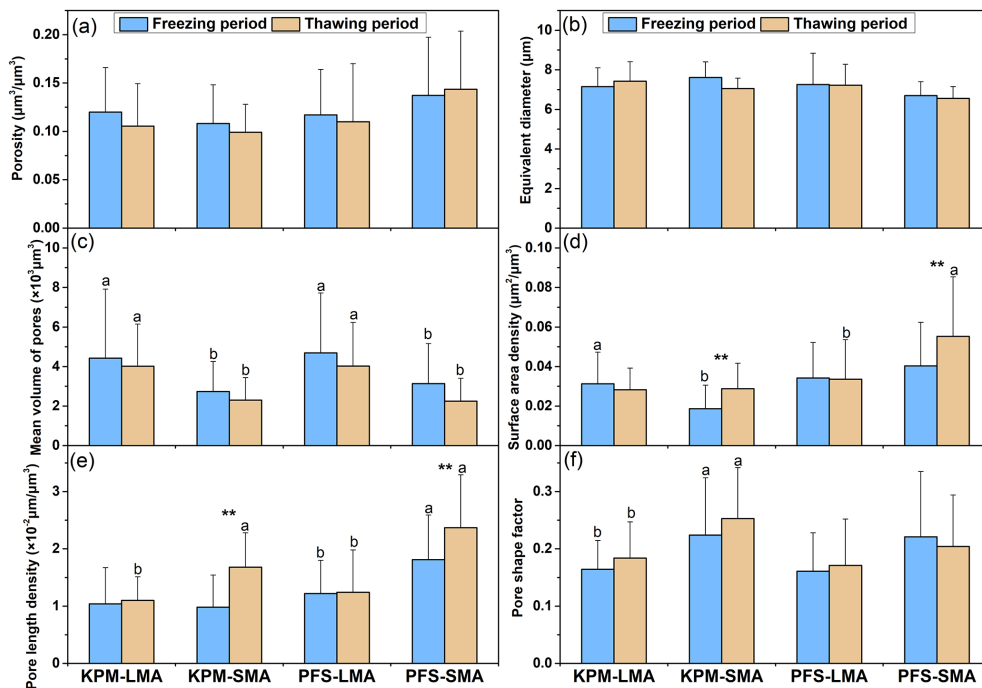


Figure 5. Pore characteristics of soil aggregates during the seasonal FT process. (a) Porosity, (b) pore equivalent diameter, (c) mean volume of pores, (d) pore surface area density, (e) pore length density and (f) pore shape factor. Bars represent the mean ± standard error ($n = 18$). The asterisks (**) represent significant differences between pore characteristics in the freezing period and the thawing period ($p < 0.05$). Different lowercase letters denote significant differences between pore characteristics of > 2 mm aggregates and 0.25 – 2 mm aggregates ($p < 0.05$). LMA: > 2 mm aggregates. SMA: 0.25 – 2 mm aggregates. KPM: the meadow ecosystem. PFS: the shrubland ecosystem.

29.99 g kg^{-1} in the stable frozen period, followed by a decline of 42.38% in the unstable thawing period (Fig. 6c). In the shrubland ecosystem, POC contents in freezing periods were significantly higher than those in thawing periods (Fig. 6b) ($p < 0.05$). The unstable thawing period was accompanied by a significant loss in MAOC compared with the stable frozen period (41.54% for > 2 mm aggregates and

39.14% for 0.25 – 2 mm aggregates) (Fig. 6c) ($p < 0.05$). Therefore, freezing is associated with SOC accumulation, and the beginning of thawing is associated with a significant loss of SOC.

The changes in the coefficient of variation (CV) of SOC content during the seasonal FT process, which depicted the variation in the SOC of aggregates from different soil depths,

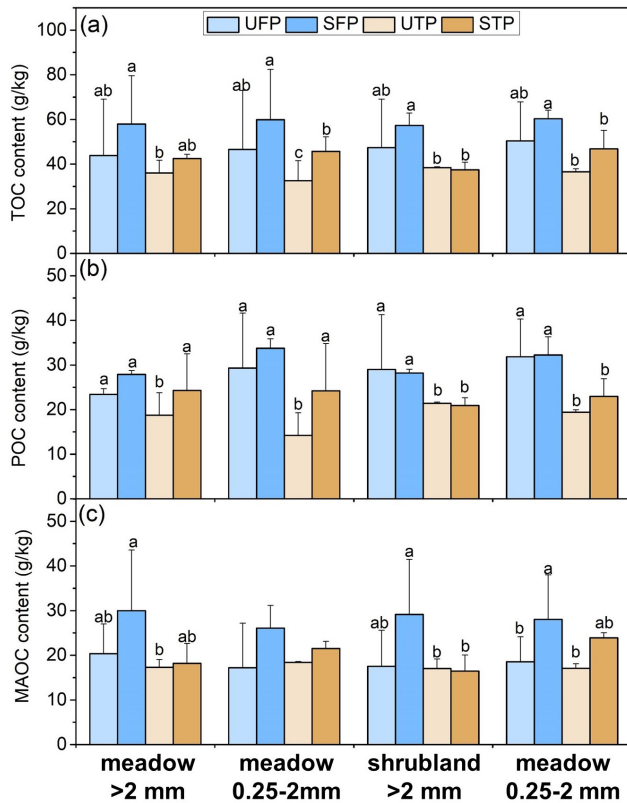


Figure 6. Changes of SOC content of soil aggregates during the seasonal FT process: (a) TOC, (b) POC and (c) MAOC. Bars represent the mean \pm standard error ($n = 9$). Different lowercase letters denote significant differences among SOC contents in different FT periods ($p < 0.05$). UFP: unstable freezing period. SFP: stable frozen period. UTP: unstable thawing period. STP: stable thawed period.

are shown in Table 1. In the two ecosystems, the CV values in the stable frozen period (0.20 for the meadow ecosystem and 0.22 for the shrubland ecosystem) were significantly lower than those in other periods ($p < 0.05$). These results revealed that the freezing process was characterized by a more uniform distribution of SOC across different soil layers.

3.3 Relationships between pore structure and SOC fractions of aggregates

In the freezing period, no correlations were observed between SOC fractions and pore parameters, while pore size distribution had significant correlations with SOC content. The TOC and MAOC contents were both positively correlated with pores of $> 80 \mu\text{m}$ (Fig. 7b) ($p = 0.039$ and $p = 0.041$, respectively) but negatively correlated with pores of $15\text{--}30 \mu\text{m}$ (Fig. 7a) ($p = 0.010$ and $p = 0.013$, respectively). In the thawing period, the POC content was positively correlated with pores of $< 15 \mu\text{m}$ ($p = 0.049$) (Fig. 8c). The TOC and MAOC contents were both positively correlated with

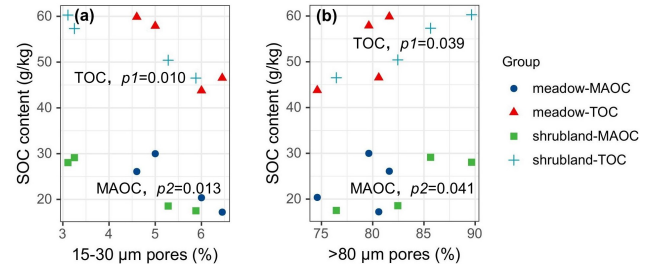


Figure 7. Scatter plots of relationships between (a) SOC content and $15\text{--}30 \mu\text{m}$ pores and (b) SOC content and $> 80 \mu\text{m}$ pores in the freezing process.

pore length density ($p = 0.045$ and $p = 0.006$, respectively) (Fig. 8a and b).

RDA was used to explain the relationship between the pore parameters and SOC fractions during the seasonal FT process (Fig. S1 in the Supplement). In the freezing period, a total of 53.29% of the SOC variation could be explained by pore characteristics. Pore EqD had a significant impact on SOC content ($p = 0.01$). In the thawing period, 52.90% of the SOC variation was explained by pore characteristics. Pore surface area density and EqD had a significant impact on the SOC of aggregates ($p = 0.01$ and $p = 0.04$, respectively).

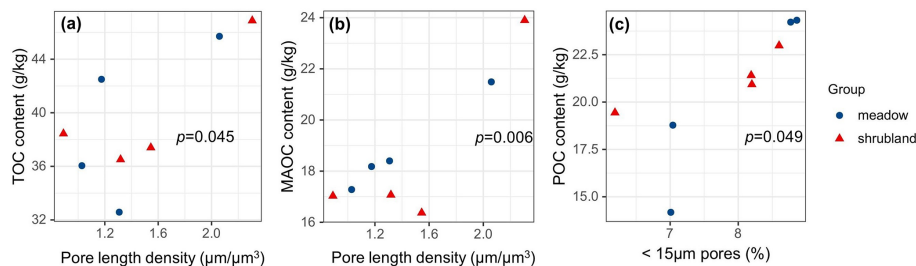
4 Discussion

Our results demonstrated that the volume percentage of $> 80 \mu\text{m}$ pores of aggregates was high in the stable frozen period. This finding is consistent with related results, which proved that FT resulted in an increase in macroporosity (Ma et al., 2021; Wu and Hu, 2024). Liu et al. (2023) reported an increase of over 200% in aggregate porosity after 15 FT cycles. Pore-scale heterogeneities result in pressure gradients and water seeping from smaller to larger pores during freezing (Rempel and van Alst, 2013), and this process enhances the expansion of force heave (Skvortsova et al., 2018). Freezing could also increase pore size by forming new connections among adjacent pores (Ma et al., 2021). The increase in pore size and porosity could loosen the aggregate stability and increase pore air content, thus increasing the air pressure and enhancing expansion (Lugato et al., 2010; de Jesus Arrieta Baldovino et al., 2021). We also found that the seasonal FT process mainly affects the pore characteristics of $0.25\text{--}2 \text{ mm}$ aggregates rather than those of $> 2 \text{ mm}$ aggregates, especially in the pore surface area density and length density. Zhao and Hu (2023a) reported a similar significant change in pore surface area density of $0.25\text{--}1 \text{ mm}$ aggregates after FT cycles. Changes in surface area density and pore length density or pores might be associated with pore shape. In the freezing period, the frost heave force of water is anisotropic, which increases the pore length and decreases the surface area (Rooney et al., 2022). Considering the variations in binding materials for aggregates with different sizes

Table 1. Coefficient of variation (CV) of SOC content of aggregates in all soil layers during the seasonal FT process.

Ecosystem	Seasonal FT periods			
	UFP	SFP	UTP	STP
Meadow	0.38 ± 0.12a	0.20 ± 0.07b	0.47 ± 0.19a	0.56 ± 0.21a
Shrubland	0.46 ± 0.16a	0.22 ± 0.09b	0.34 ± 0.17a	0.34 ± 0.13a

Bars represent the mean ± standard error ($n = 6$). Different lowercase letters denote significant differences in the CV of different FT periods. UFP: unstable freezing period. SFP: stable frozen period. UTP: unstable thawing period. STP: stable thawed period.

**Figure 8.** Scatter plots of relationships between (a) TOC content and pore length density, (b) MAOC content and pore length density, and (c) POC content and < 15 μm pores in the thawing process.

(Tisdall and Oades, 1982), as well as the complex process of pore formation in alpine regions (Zhao et al., 2020), quantifying the pore network of different aggregates can help better evaluate their carbon protection ability, and this requires further investigations.

In our study, contents of SOC fractions were all high in the stable frozen period and low in the unstable thawing period. Huang et al. (2021) found that the TOC content of aggregates was high in January and February, followed by a significant decline in March due to FT processes. Many studies have also reported the SOC loss at the beginning of the thawing period at regional scales (Song et al., 2017, 2020). This phenomenon can be explained by litter accumulation and suppressed microbial activities in freezing periods (Han et al., 2018), as well as the aerobic environment intensifying SOC mineralization during thawing (Liu et al., 2018, 2021). So, the freezing process is characterized by SOC accumulation, while the thawing process is associated with SOC loss. The freezing process was also accompanied by a more uniform distribution of SOC across different soil layers. This finding corresponds to Zhao and Hu (2023b), who proposed that freezing buffered the difference in microbial biomass between soil horizons. Apart from seasonal dynamics in phenology and hydrology, differences in external disturbances and SOC turnover rates from topsoil to deep soil also contributed to this phenomenon (Sun et al., 2020; Wang et al., 2022). Therefore, freezing might pose an indirect and positive impact on vertical nutrient distribution, which has lacked investigation so far.

Among all pore characteristics, equivalent diameter explained most in the SOC variations. In the freezing period,

pores of 15–30 μm had a negative impact on SOC protection; this was consistent with our previous results (Wang and Hu, 2023). Pores of 15–30 μm are probably a suitable habitat for soil microbes that supports their activity, where greater SOC decomposition takes place (Kravchenko and Guber, 2017; Liang et al., 2019). Pores of > 80 μm might contribute to SOC protection of aggregates. As the period was characterized by SOC accumulation (especially residue entry), pores of > 80 μm serve as primary sites for residue entry and are promoted by microbial materials and SOC, which enhance soil aggregation and thus drive much SOC to be protected (Ananyeva et al., 2013; Dal Ferro et al., 2014; Zhang et al., 2023). Freezing promoted the formation of these pores which were conducive to organic matter entry into aggregates. In the thawing period, pores of < 15 μm were positively correlated with SOC content. Previous studies proved that these pores inhibited SOC loss via limiting microbial access and shifting microbial metabolism to less efficient anaerobic respiration (Strong et al., 2004; Keiluweit et al., 2017). On the QTP, the positive impact of soil moisture on SOC protection has been revealed on both the aggregate scale and the landscape scale (Ma et al., 2022; Wang and Hu, 2023). The thawing process is accompanied by an increase in microbial activity and moisture availability; pores of < 15 μm are able to hold water surrounding the soil particles (Kim et al., 2021). Therefore, POC associated with these pores was less vulnerable to microbial processing and desorption as thawing enhanced the exchanged soil solution and consequent equilibration (Schluter et al., 2022). The protection promotes the consequent transport of POC towards mineral sorption sites and thus contributes to the long-term SOC storage (Védère

et al., 2020). Overall, the FT-induced pore structure could pose a positive impact on SOC protection in that pores of $> 80 \mu\text{m}$ promoted by freezing might serve as primary sites for organic matter entry, while pores of $< 15 \mu\text{m}$ promoted by thawing were positively associated with POC protection through holding moisture.

In this study, we explored changes in the pore structure and SOC fractions of alpine soil aggregates during the seasonal FT process. However, we could not isolate the impact of FT processes on soil structure and functions as impacts from vegetation and climate could not be avoided under field conditions. Therefore, it is necessary to compare the results based on laboratory FT simulations and field sampling in future studies to clarify the importance of FT processes in shaping pore structure and affecting soil functions. Despite the difficulty in in situ monitoring, soil respiration measurements and DOC measurements would be a more direct way to capture the loss pathways of SOC exerted by thawing. Also, recent studies have clarified the importance of minerals (e.g., Fe, Al and their oxides) in microscale SOC protection (Kang et al., 2024; Wang et al., 2024; Zhu et al., 2024). For example, the presence of iron-rich substances can hamper microbial degradation of organic compounds, and the iron-bound organic carbon (Fe-OC) accounted for approximately 20% of the total carbon pool on the QTP (Mu et al., 2016). This mechanism can be closely associated with soil moisture and enzyme activities, both of which are altered by FT processes (Li et al., 2023; Hu et al., 2024), while the role of pore structure has not been clarified. Future research needs to further quantify the impact of soil structure on organic carbon, which will enable us to apply the mechanisms we have discovered to landscape scales to improve existing global carbon cycle predictions.

5 Conclusion

The findings of the study revealed that seasonal FT processes regulate pore structure and SOC concentration of aggregates. Pore surface area density and length density of 0.25–2 mm aggregates changed significantly during the seasonal FT process. The freezing period promoted the formation of pores $> 80 \mu\text{m}$, while thawing could lead to shrinkage of pore space. Freezing is featured by accumulation of SOC of aggregates and the more uniform distribution of SOC among different soil layers. Thawing witnessed the loss of SOC. The seasonal FT process could promote the SOC protection of aggregates via regulating pore size distribution. Pores of $> 80 \mu\text{m}$ promoted by freezing might serve as primary sites for organic matter entry, while pores of $< 15 \mu\text{m}$ promoted by thawing could inhibit POC decomposition through holding moisture. Overall, our study explains the changes in SOC during the freeze–thaw process by innovatively establishing a potential mechanism of how FT processes regulate pore structure and SOC. In future studies, by incorporating more

of a variety of factors with in situ monitoring, we hope the contribution of soil structure to SOC conservation can be up-scaled to achieve a more precise global carbon cycle estimation.

Appendix A: Abbreviations

FT	freeze–thaw
UFP	unstable freezing period
SFP	stable frozen period
UTP	unstable thawing period
STP	stable thawed period
EqD	equivalent diameter of pores
SF	shape factor
LMA	large macroaggregate
SMA	small macroaggregate
SOC	soil organic carbon
TOC	total organic carbon
POC	particulate organic carbon
MAOC	mineral-associated organic carbon
DOC	dissolved organic carbon
TN	total nitrogen

Data availability. All data generated or analysed during this study are included in this published article and its supplement.

Supplement. The supplement related to this article is available online at: <https://doi.org/10.5194/soil-10-859-2024-supplement>.

Author contributions. RW: conceptualization, data curation, formal analysis, methodology, writing (original draft), writing (review and editing). XH: funding acquisition, investigation, project administration, supervision, writing (review and editing).

Competing interests. The contact author has declared that neither of the authors has any competing interests.

Disclaimer. Publisher's note: Copernicus Publications remains neutral with regard to jurisdictional claims made in the text, published maps, institutional affiliations, or any other geographical representation in this paper. While Copernicus Publications makes every effort to include appropriate place names, the final responsibility lies with the authors.

Financial support. This study was financially supported by the National Natural Science Foundation of China (grant no. 42371107).

Review statement. This paper was edited by Hu Zhou and reviewed by two anonymous referees.

References

- Ananyeva, K., Wang, W., Smucker, A. J. M., Rivers, M. L., and Kravchenko, A. N.: Can intra-aggregate pore structures affect the aggregate's effectiveness in protecting carbon?, *Soil Biol. Biochem.*, 57, 868–875, <https://doi.org/10.1016/j.soilbio.2012.10.019>, 2013.
- Cambardella, C. A. and Elliott, E. T.: Particulate soil organic-matter changes across a grassland cultivation sequence, *Soil Sci. Soc. Am. J.*, 56, 777–783, <https://doi.org/10.2136/sssaj1992.03615995005600030017x>, 1992.
- Campbell, J. L., Soccia, A. M., and Templer, P. H.: Increased nitrogen leaching following soil freezing is due to decreased root uptake in a northern hardwood forest, *Glob. Change Biol.*, 20, 2663–2673, <https://doi.org/10.1111/gcb.12532>, 2014.
- Chen, H., Liu, X., Xue, D., Zhu, D., Zhan, W., Li, W., Wu, N., and Yang, G.: Methane emissions during different freezing–thawing periods from a fen on the Qinghai–Tibet Plateau: Four years of measurements, *Agr. Forest Meteorol.*, 297, 108279, <https://doi.org/10.1016/j.agrformet.2020.108279>, 2021.
- Chen, J., Xiao, W., Zheng, C., and Zhu, B.: Nitrogen addition has contrasting effects on particulate and mineral-associated soil organic carbon in a subtropical forest, *Soil Biol. Biochem.*, 142, 107708, <https://doi.org/10.1016/j.soilbio.2020.107708>, 2020.
- Dagesse, D. F.: Freezing cycle effects on water stability of soil aggregates, *Can. J. Soil. Sci.*, 93, 473–483, <https://doi.org/10.4141/CJSS2012-046>, 2013.
- Dal Ferro, N., Sartori, L., Simonetti, G., Berti, A., and Morari, F.: Soil macro- and microstructure as affected by different tillage systems and their effects on maize root growth, *Soil Till. Res.*, 140, 55–65, <https://doi.org/10.1016/j.still.2014.02.003>, 2014.
- de Jesus Arrieta Baldovino, J., dos Santos Izzo, R. L., and Rose, J. L.: Effects of freeze–thaw cycles and porosity/cement index on durability, strength and capillary rise of a stabilized silty soil under optimal compaction conditions, *Geotech. Geol. Eng.*, 39, 481–498, <https://doi.org/10.1007/s10706-020-01507-y>, 2021.
- Deng, Y., Li, X., Shi, F., and Zhang, Y.: Divergent controlling factors of freeze–thaw-induced changes in dissolved organic carbon and microbial biomass carbon between topsoil and subsoil of cold alpine grasslands, *Catena*, 241, 108063, <https://doi.org/10.1016/j.catena.2024.108063>, 2024.
- Estop-Aragonés, C., Olefeldt, D., Abbott, B. W., Chanton, J. P., Czimczik, C. I., Dean, J. F., Egan, J. E., Gandois, L., Garnett, M. H., Hartley, I. P., Hoyt, A., Lupascu, M., Natali, S. M., O'Donnell, J. A., Raymond, P. A., Tanentzap, A. J., Tank, S. E., Schuur, E. A. G., Turetsky, M., and Anthony, K. W.: Assessing the Potential for Mobilization of Old Soil Carbon After Permafrost Thaw: A Synthesis of ^{14}C Measurements from the Northern Permafrost Region, *Global Biogeochem. Cy.*, 34, 1–26, <https://doi.org/10.1029/2020GB006672>, 2020.
- Fu, C., Li, Y., Zeng, L., Tu, C., Wang, X., Ma, H., Xiao, L., Christie, P., and Luo, Y.: Climate and mineral accretion as drivers of mineral-associated and particulate organic matter accumulation in tidal wetland soils, *Glob. Change Biol.*, 30, e17070, <https://doi.org/10.1111/gcb.17070>, 2023.
- Gao, Z., Hu, X., Li, X., and Li, Z.: Effects of freeze–thaw cycles on soil macropores and its implications on formation of hummocks in alpine meadows in the Qinghai Lake watershed, north-eastern Qinghai–Tibet Plateau, *J. Soils Sediments*, 21, 245–256, <https://doi.org/10.1007/s11368-020-02765-2>, 2021.
- Han, C., Gu, Y., Kong, M., Hu, L., Jia, Y., Li, F., Sun, G., and Siddique, K. H. M.: Responses of soil microorganisms, carbon and nitrogen to freeze–thaw cycles in diverse land-use types, *Appl. Soil Ecol.*, 124, 211–217, <https://doi.org/10.1016/j.apsoil.2017.11.012>, 2018.
- He, L., Lai, C., Mayes, M. A., Murayama, S., and Xu, X.: Microbial seasonality promotes soil respiratory carbon emission in natural ecosystems: a modelling study, *Glob. Change Biol.*, 27, 3035–3051, <https://doi.org/10.1111/gcb.15627>, 2021.
- Henry, H. A. L.: Seasonal freeze–thaw cycle experiments: Trends, methodological weaknesses and suggested improvements, *Soil Biol. Biochem.*, 39, 977–986, <https://doi.org/10.1016/j.soilbio.2006.11.017>, 2007.
- Hu, W., Li, Q., Wang, W., Lin, X., He, Z., and Li, G.: Straw mulching decreased the contribution of Fe-bound organic carbon to soil organic carbon in a banana orchard, *Appl. Soil Ecol.*, 194, 105177, <https://doi.org/10.1016/j.apsoil.2023.105177>, 2024.
- Hu, X., Li, Z., Li, X., and Liu, L.: Quantification of soil macropores under alpine vegetation using computed tomography in the Qinghai Lake Watershed, NE Qinghai–Tibet Plateau, *Geoderma*, 264, 244–251, <https://doi.org/10.1016/j.geoderma.2015.11.001>, 2016.
- Hu, X., Jiang, L., Zhao, Y., and Li, X.: Characteristics of the soil macropore and root architecture of alpine meadows during the seasonal freezing–thawing process and their impact on water transport in the Qinghai Lake watershed, northeastern Qinghai–Tibet Plateau, *J. Soil Water Conserv.*, 78, 299–308, <https://doi.org/10.2489/jswc.2023.00155>, 2023.
- Huang, D., Zhou, L., Fan, H., Jia, Y., and Liu, M.: Responses of aggregates and associated soil available phosphorus, and soil organic matter in different slope aspects, to seasonal freeze–thaw cycles in Northeast China, *Geoderma*, 402, 115184, <https://doi.org/10.1016/j.geoderma.2021.115184>, 2021.
- IUSS Working Group WRB: World Reference Base for Soil Resources, International soil classification system for naming soils and creating legends for soil maps, 4th edn., International Union of Soil Sciences (IUSS), Vienna, Austria, ISBN 979-8-9862451-1-9, 2022.
- Jaques, V. A. J., Du Plessis, A., Zemek, M., Salplachta, J., Stubianova, Z., Zikmund, T., and Kaiser, J.: Review of porosity uncertainty estimation methods in computed tomography dataset, *Meas. Sci. Technol.*, 32, 122001, <https://doi.org/10.1088/1361-6501/ac1b40>, 2021.
- Kang, J., Qu, C., Chen, W., Cai, P., Chen, C., and Huang, Q.: Organo-organic interactions dominantly drive soil organic carbon accrual, *Glob. Change Biol.*, 30, e17147, <https://doi.org/10.1111/gcb.17147>, 2024.
- Keiluweit, M., Wanzek, T., Kleber, M., Nico, P., and Fendorf, S.: Anaerobic microsites have an unaccounted role in soil carbon stabilization, *Nat Commun.*, 8, 1771, <https://doi.org/10.1038/s41467-017-01406-6>, 2017.
- Kim, Y., Hyun, J., Yoo, S., and Yoo, J.: The role of biochar in alleviating soil drought stress in urban roadside greenery, *Geoderma*,

- 404, 115223, <https://doi.org/10.1016/j.geoderma.2021.115223>, 2021.
- Kim, Y. J., Kim, J., and Jung, J. Y.: Responses of dissolved organic carbon to freeze–thaw cycles associated with the changes in microbial activity and soil structure, *The Cryosphere*, 17, 3101–3114, <https://doi.org/10.5194/tc-17-3101-2023>, 2023.
- Klute, A.: *Methods of Soil Analysis: Part 1 – Physical and Mineralogical Methods*, American Society of Agronomy, Madison, ISBN 9780891188643, 1986.
- Kravchenko, A. N. and Guber, A. K.: Soil pores and their contributions to soil carbon processes, *Geoderma*, 287, 31–39, <https://doi.org/10.1016/j.geoderma.2016.06.027>, 2017.
- Kravchenko, A. N., Guber, A. K., Razavi, B. S., Koestel, J. K., Quigley, M. Y., Robertson, G. P., and Kuzyakov, Y.: Microbial spatial footprint as a driver of soil carbon stabilization, *Nat. Commun.*, 10, 3121, <https://doi.org/10.1038/s41467-019-11057-4>, 2019.
- Kravchenko, A. N., Negassa, W. C., Guber, A. K., and Rivers, M. L.: Protection of soil carbon within macro-aggregates depends on intra-aggregate pore characteristics, *Sci. Rep.*, 5, 1–10, <https://doi.org/10.1038/srep16261>, 2015.
- Kreyling, J., Beierkuhnlein, C., Pirtsch, K., Schloter, M., and Jentsch, A.: Recurrent soil freeze-thaw cycles enhance grassland productivity, *New Phytol.*, 177, 938–945, <https://doi.org/10.1111/j.1469-8137.2007.02309.x>, 2007.
- Lal, R. and Shukla, M. K.: *Principles of Soil physics*, Marcel Dekker, New York, ISBN 0-8247-5324-0, 2004.
- Li, G. and Fan, H.: Effect of freeze-thaw on water stability of aggregates in a black soil of Northeast China, *Pedosphere*, 24, 285–290, [https://doi.org/10.1016/S1002-0160\(14\)60015-1](https://doi.org/10.1016/S1002-0160(14)60015-1), 2014.
- Li, P., Kong, D., Zhang, H., Xu, L., Li, C., Wu, M., Jiao, J., Li, D., Xu, L., Li, H., and Hu, F.: Different regulation of soil structure and resource chemistry under animal-and plant- derived organic fertilizers changed soil bacterial communities, *Appl. Soil Ecol.*, 165, 104020, <https://doi.org/10.1016/j.apsoil.2021.104020>, 2022.
- Li, R., Luo, H., Yu, J., Luo, Y., He, Y., Deng, S., Deng, O., Shi, D., He, J., Xiao, H., Wang, L., and Lan, T.: The importance of moisture in regulating soil organic carbon content based on a comparison of “enzymic latch” and “iron gate” in Zoige Plateau peatland, *Catena*, 225, 107019, <https://doi.org/10.1016/j.catena.2023.107019>, 2023.
- Li, X., Yang, X., Ma, Y., Hu, G., Hu, X., Wu, X., Wang, P., Huang, Y., Cui, B., and Wei, J.: Qinghai Lake Basin critical zone observatory on the Qinghai-Tibet Plateau, *Vadose Zone J.*, 17, 180069, <https://doi.org/10.2136/vzj2018.04.0069>, 2018.
- Liang, A., Zhang, Y., Zhang, X., Yang, X., McLaughlin, N., Chen, X., Guo, Y., Jia, S., Zhang, S., Wang, L., and Tang, J.: Investigations of relationships among aggregate pore structure, microbial biomass, and soil organic carbon in a Molisol using combined non-destructive measurements and phospholipid fatty acid analysis, *Soil Till. Res.*, 185, 94–101, <https://doi.org/10.1016/j.still.2018.09.003>, 2019.
- Lin, Z., Gao, Z., Niu, F., Luo, J., Yin, G., Liu, M., and Fan, X.: High spatial density ground thermal measurements in a warming permafrost region, Beiluhe Basin, Qinghai-Tibet Plateau, *Geomorphology*, 340, 1–14, <https://doi.org/10.1016/j.geomorph.2019.04.032>, 2019.
- Liu, B., Fan, H., Jiang, Y., and Ma, R.: Evaluation of soil macro-aggregate characteristics in response to soil macropore characteristics investigated by X-ray computed tomography under freeze-thaw effects, *Soil Till. Res.*, 225, 105559, <https://doi.org/10.1016/j.still.2022.105559>, 2023.
- Liu, F., Chen, L., Abbott, B. W., Xu, Y., Yang, G., Kou, D., Qin, S., Strauss, J., Wang, Y., Zhang, B., and Yang, Y.: Reduced quantity and quality of SOM along a thaw sequence on the Tibetan Plateau, *Environ. Res. Lett.*, 13, 104017, <https://doi.org/10.1088/1748-9326/aae43b>, 2018.
- Liu, F., Kou, D., Chen, Y., Xue, K., Ernakovic, J. G., Chen, L., Yang, G., and Yang, Y.: Altered microbial structure and function after thermokarst formation, *Glob. Change Biol.*, 27, 823–835, <https://doi.org/10.1111/gcb.15438>, 2021.
- Lugato, E., Morari, F., and Nardi, S.: Relationship between aggregate pore size distribution and organic-humic carbon in contrasting soils, *Soil Till. Res.*, 103, 153–157, <https://doi.org/10.1016/j.still.2008.10.013>, 2009.
- Lugato, E., Simonetti, G., Morari, F., Nardi, S., Berti, A., and Giardini, L.: Distribution of organic and humic carbon in wet-sieved aggregates of different soils under long-term fertilization experiment, *Geoderma*, 157, 80–85, <https://doi.org/10.1016/j.geoderma.2010.03.017>, 2010.
- Ma, R., Jiang, Y., Liu, B., and Fan, H.: Effects of pore structure characterized by synchrotron-based micro-computed tomography on aggregate stability of black soil under freeze-thaw cycles, *Soil Till. Res.*, 207, 104855, <https://doi.org/10.1016/j.still.2020.104855>, 2021.
- Ma, Y., Xie, T., and Li, X.: Spatial variation of soil organic carbon in the Qinghai Lake watershed, north-east Qinghai-Tibet Plateau, *Catena*, 213, 106187, <https://doi.org/10.1016/j.catena.2022.106187>, 2022.
- Mako, A., Szabo, B., Rajkai, K., Szabo, J., Bakacsi, Z., Labancz, V., Hernadi, H., and Barna, G.: Evaluation of soil texture determination using soil fraction data resulting from laser diffraction method, *Int. Agrophys.*, 33, 445–454, <https://doi.org/10.31545/intagr/113347>, 2019.
- Mu, C., Zhang, T., Zhao, Q., Guo, H., Zhong, W., Su, H., and Wu, Q.: Soil organic carbon stabilization by iron in permafrost regions of the Qinghai-Tibet Plateau, *Geophys. Res. Lett.*, 43, 10286–10294, <https://doi.org/10.1002/2016GL070071>, 2016.
- Ozlu, E. and Arriaga, F. J.: The role of carbon stabilization and minerals on soil aggregation in different ecosystems, *Catena*, 202, 105303, <https://doi.org/10.1016/j.catena.2021.105303>, 2021.
- Oztas, T. and Fayetorbay, F.: Effect of freezing and thawing processes on soil aggregate stability, *Catena*, 52, 1–8, [https://doi.org/10.1016/S0341-8162\(02\)00177-7](https://doi.org/10.1016/S0341-8162(02)00177-7), 2003.
- Patel, K. F., Tatariw, C., Macrae, J. D., Ohno, T., Nelson, S. J., and Fernandez, I. J.: Repeated freeze-thaw cycles increase extractable, but not total, carbon and nitrogen in a Maine coniferous soil, *Geoderma*, 402, 115353, <https://doi.org/10.1016/j.geoderma.2021.115353>, 2021.
- Peng, X., Zhang, T., Frauenfeld, O. W., Wang, K., Cao, B., Zhong, X., Su, H., and Mu, C.: Response of seasonal soil freeze depth to climate change across China, *The Cryosphere*, 11, 1059–1073, <https://doi.org/10.5194/tc-11-1059-2017>, 2017.
- Qiao, L., Zhou, H., Wang, Z., Li, Y., Chen, W., Wu, Y., Liu, G., and Xue, S.: Variations in soil aggregate stability and organic carbon stability of alpine meadow and

- shrubland under long-term warming, *Catena*, 222, 106848, <https://doi.org/10.1016/j.catena.2022.106848>, 2023.
- Quigley, M. Y. and Kravchenko, A. N.: Inputs of root-derived carbon into soil and its losses are associated with pore-size distributions, *Geoderma*, 410, 115667, <https://doi.org/10.1016/j.geoderma.2021.115667>, 2022.
- Rabot, E., Wiesmeier, M., Schlute, S., and Vogel, H. J.: Soil structure as an indicator of soil functions: A review, *Geoderma*, 314, 122–137, <https://doi.org/10.1016/j.geoderma.2017.11.009>, 2018.
- Rempel, A. W. and van Alst, L. J.: Potential gradients produced by pore-space heterogeneities: Application to isothermal frost damage and submarine hydrate anomalies, *Poromechanics V*, 813–822, <https://doi.org/10.1061/9780784412992.098>, 2013.
- Rooney, E. C., Bailey, V. L., Patel, K. F., Dragila, M., Battu, A. K., Buchko, A. C., Gallo, A. C., Hatten, J., Possinger, A. R., Qafoku, O., Reno, L. R., SanClements, M., Varga, T., and Lybrand, R. A.: Soil pore network response to freeze-thaw cycles in permafrost aggregates, *Geoderma*, 411, 115674, <https://doi.org/10.1016/j.geoderma.2021.115674>, 2022.
- Ruamps, L. S., Nunan, N., Pouteau, V., Leloup, J., Raynaud, X., Roy, V., and Chenu, C.: Regulation of soil organic C mineralisation at the pore scale, *FEMS Microbiol. Ecol.*, 86, 26–35, <https://doi.org/10.1111/1574-6941.12078>, 2013.
- Schluter, S., Leuther, F., Albrecht, L., Hoeschen, C., Kilian, R., Surey, R., Mikutta, R., Kaiser, K., Mueller, C. W., and Vogel, H.: Microscale carbon distribution around pores and particulate organic matter varies with soil moisture regime, *Nat. Commun.*, 13, 2098, <https://doi.org/10.1038/s41467-022-29605-w>, 2022.
- Schutter, M. E. and Dick, R. P.: Microbial community profiles and activities among aggregates of winter fallow and cover-cropped soil, *Soil Sci. Soc. Am. J.*, 66, 142–153, <https://doi.org/10.2136/sssaj2002.1420>, 2002.
- Schuur, E. A. G. and Mack, M. C.: Ecological response to permafrost thaw and consequences for local and global ecosystem services, *Annu. Rev. Ecol. Evol.*, 49, 279–301, <https://doi.org/10.1146/annurev-ecolsys-121415-032349>, 2018.
- Six, J., Elliott, E. T., Paustian, K., and Doran, J. W.: Aggregation and soil organic matter accumulation in cultivated and native grassland soils, *Soil Sci. Soc. Am. J.*, 62, 1367–1377, <https://doi.org/10.2136/sssaj1998.03615995006200050032x>, 1998.
- Skvortsova, E. B., Shen, E. V., and Abrosimov, K. N.: The impact of multiple freeze-thaw cycles on the microstructure of aggregates from a Soddy-Podzolic soil: a microtomographic analysis, *Eurasian Soil Sci.*, 51, 190–198, <https://doi.org/10.1134/S1064229318020102>, 2018.
- Song, X., Wang, G., Ran, F., Huang, K., Sun, J., and Song, C.: Soil moisture as a key factor in carbon release from thawing permafrost in a boreal forest, *Geoderma*, 357, 113975, <https://doi.org/10.1016/j.geoderma.2019.113975>, 2020.
- Song, Y., Zou, Y., Wang, G., and Yu, X.: Altered soil carbon and nitrogen cycles due to the freeze-thaw effect: A meta-analysis, *Soil Biol. Biochem.*, 109, 35–49, <https://doi.org/10.1016/j.soilbio.2017.01.020>, 2017.
- Starkloff, T., Larsbo, M., Stolte, J., Hessel, R., and Ritsema, C.: Quantifying the impact of a succession of freezing-thawing cycles on the pore network of a silty clay loam and a loamy sand topsoil using X-ray tomography, *Catena*, 156, 365–374, <https://doi.org/10.1016/j.catena.2017.04.026>, 2017.
- Strong, E. T., Wever, H. D., Merckx, R., and Recous, S.: Spatial location of carbon decomposition in the soil pore system, *Eur. J. Soil Sci.*, 55, 739–750, <https://doi.org/10.1111/j.1365-2389.2004.00639.x>, 2004.
- Sun, T., Mao, X., Han, K., Wang, X., Cheng, Q., Liu, X., Zhou, J., Ma, Q., Ni, Z., and Wu, L.: Nitrogen addition increased soil particulate organic carbon via plant carbon input whereas reduced mineral-associated organic carbon through attenuating mineral protection in agroecosystem, *Sci. Total Environ.*, 899, 165705, <https://doi.org/10.1016/j.scitotenv.2023.165705>, 2023.
- Sun, T., Wang, Y., Hui, D., Jing, X., and Feng, W.: Soil properties rather than climate and ecosystem type control the vertical variations of soil organic carbon, microbial carbon, and microbial quotient, *Soil Biol. Biochem.*, 148, 107905, <https://doi.org/10.1016/j.soilbio.2020.107905>, 2020.
- Tan, B., Wu, F., Yang, W., and He, X.: Snow removal alters soil microbial biomass and enzyme activity in a Tibetan alpine forest, *Appl. Soil Ecol.*, 76, 34–41, <https://doi.org/10.1016/j.apsoil.2013.11.015>, 2014.
- Tarnocai, C., Canadell, J. G., Schuur, E. A. G., Kuhry, P., Mazhitova, G., and Zimov, S.: Soil organic carbon pools in the northern circumpolar permafrost region, *Global Biogeochem. Cy.*, 23, GB2023, <https://doi.org/10.1029/2008GB003327>, 2009.
- Tisdall, J. M. and Oades, J. M.: Organic-matter and water-stable aggregates in soils, *J. Soil Sci.*, 33, 141–163, <https://doi.org/10.1111/j.1365-2389.1982.tb01755.x>, 1982.
- Védère, C., Vieublé Gonod, L., Pouteau, V., Girardin, C., and Chenu, C.: Spatial and temporal evolution of detritusphere hotspots at different soil moistures, *Soil Biol. Biochem.*, 150, 107975, <https://doi.org/10.1016/j.soilbio.2020.107975>, 2020.
- Wang, D., Ma, Y., Niu, Y., Chang, X., and Wen, Z.: Effects of cyclic freezing and thawing on mechanical properties of Qinghai-Tibet clay, *Cold Reg. Sci. Tech.*, 48, 34–43, <https://doi.org/10.1016/j.coldregions.2006.09.008>, 2007.
- Wang, E., Cruse, R., Chen, X., and Daigh, A.: Effects of moisture condition and freeze/thaw cycles on surface soil aggregate size distribution and stability, *Can. J. Soil Sci.*, 92, 529–536, <https://doi.org/10.1007/s40333-017-0009-3>, 2012.
- Wang, M., Guo, X., Zhang, S., Xiao, L., Mishra, U., Yang, Y., Zhu, B., Wang, G., Mao, X., Qian, T., Jiang, T., Shi, Z., and Luo, Z.: Global soil profiles indicate depth-dependent soil carbon losses under a warmer climate, *Nat. Commun.*, 13, 5514, <https://doi.org/10.1038/s41467-022-33278-w>, 2022.
- Wang, R. and Hu, X.: Pore structure characteristics and organic carbon distribution of soil aggregates in alpine ecosystems in the Qinghai Lake basin on the Qinghai-Tibet Plateau, *Catena*, 231, 107359, <https://doi.org/10.1016/j.catena.2023.107359>, 2023.
- Wang, X., Wang, C., and Fan, X.: Mineral composition controls the stabilization of microbially derived carbon and nitrogen in soils: Insights from an isotope tracing model, *Glob. Change Biol.*, 30, e17156, <https://doi.org/10.1111/gcb.17156>, 2024.
- Wang, Y., Li, S., and Xu, Y.: Incorporated maize residues will induce more accumulation of new POC in HF compared with that in LF soils: a comparison of different residue types, *J. Soil Sediments*, 20, 3941–3950, <https://doi.org/10.1007/s11368-020-02718-9>, 2020.

- Witzgall, K., Vidal, A., Schubert, D. I., Hoschen, C., Schweizer, S. A., Buegger, F., Pouteau, V., Chenu, C., and Mueller, C. W.: Particulate organic matter as a functional soil component for persistent soil organic carbon, *Nat. Commun.*, 12, 1–10, <https://doi.org/10.1038/s41467-021-24192-8>, 2021.
- Wu, T., Li, X., Zuo, F., Deng, Y., and Hu, G.: Responses of soil water dynamics to precipitation events in an alpine meadow ecosystem of the Qinghai Lake Basin based on high-precision lysimeter measurements, *Hydrol. Process.*, 37, e14874, <https://doi.org/10.1002/hyp.14874>, 2023.
- Wu, Y. and Hu, X.: Soil open pore structure regulates soil organic carbon fractions of soil aggregates under simulated freeze-thaw cycles as determined by X-ray computed tomography, *J. Soil Sci. Plant Nutr.*, 24, 5235–5248, <https://doi.org/10.1007/s42729-024-01904-9>, 2024.
- Xiao, L., Zhang, Y., Li, P., Xu, G., Shi, P., and Zhang, Y.: Effects of freeze-thaw cycles on aggregate-associated organic carbon and glomalin-related soil protein in natural-succession grassland and Chinese pine forest on the Loess Plateau, *Geoderma*, 334, 1–8, <https://doi.org/10.1016/j.geoderma.2018.07.043>, 2019.
- Yang, Z., Hu, X., Gao, Z., and Zhao, Y.: Soil macropore networks derived from X-ray computed tomography in response to typical thaw slumps in Qinghai-Tibetan Plateau, China, *J. Soil Sediment*, 21, 2845–2854, <https://doi.org/10.1007/s11368-021-02983-2>, 2021.
- Zhang, W., Munkholm, L. J., Liu, X., An, T., Xu, Y., Ge, Z., Xie, N., Li, A., Dong, Y., Peng, C., Li, S., and Wang, J.: Soil aggregate microstructure and microbial community structure mediate soil organic carbon accumulation: Evidence from one-year field experiment, *Geoderma*, 430, 116324, <https://doi.org/10.1016/j.geoderma.2023.116324>, 2023.
- Zhang, X., Xin, X., Zhu, A., Zhang, J., and Yang, W.: Effects of tillage and residue managements on organic C accumulation and soil aggregation in a sandy loam soil of the North China Plain, *Catena*, 156, 176–183, <https://doi.org/10.1016/j.catena.2017.04.012>, 2017.
- Zhao, Y. and Hu, X.: A pore-scale investigation of soil aggregate structure responding to freeze-thaw cycles using X-ray computed microtomography, *J. Soil Sediment*, 23, 3137–3148, <https://doi.org/10.1007/s11368-023-03539-2>, 2023a.
- Zhao, Y. and Hu, X.: Seasonal freeze-thaw processes regulate and buffer the distribution of microbial communities in soil horizons, *Catena*, 231, 107348, <https://doi.org/10.1016/j.catena.2023.107348>, 2023b.
- Zhao, Y., Hu, X., and Li, X.: Analysis of the intra-aggregate pore structures in three soil types using X-ray computed tomography, *Catena*, 193, 104622, <https://doi.org/10.1016/j.catena.2020.104622>, 2020.
- Zhou, H., Peng, X., Peth, S., and Xiao, T.: Effects of vegetation restoration on soil aggregate microstructure quantified with synchrotron-based micro-computed tomography, *Soil Till. Res.*, 124, 17–23, <https://doi.org/10.1016/j.still.2012.04.006>, 2012.
- Zhu, E., Li, Z., and Ma, L.: Enhanced mineral preservation rather than microbial residue production dictates the accrual of mineral-associated organic carbon along a weathering gradient, *Geophys. Res. Lett.*, 51, e2024GL108466, <https://doi.org/10.1029/2024GL108466>, 2024.